Authors	Title	Journal	Volume	Pages	Year
*Kokubo Y, Nakamura S, Okamura T, Yoshimasa Y, Makino H, Watanabe M, Higashiyama A, Kamide K, Kawanishi K, Okayama A, Kawano Y.	Relationship between blood pressure category and the incidence of stroke and myocardial infarction in an urban Japanese population with and without chronic kidney disease.	Stroke	40	2674-2679	2009
河野雄平	家庭血圧，24時間血圧を実地臨床に活かす	医学のあゆみ	230	408-412	2009
Tanaka H, Munakata M, Kawano Y, Ohishi M, Shoji T, Sugawara J, Tomiyama H, Yamashina A, Yasuda H, Sawayama T, Ozawa T.	Comparison between carotid-femoral and brachial-ankle pulse wave velocity as measures of arterial stiffness.	J Hypertens.	27	2022-2027	2009
*Iwashima Y, Horio T, Kamide K, Tokudome T, Yoshihara F, Nakamura S, Ogihara T, Rakugi H, Kawano Y.	Additive interaction of metabolic syndrome and chronic kidney disease on cardiac hypertrophy and risk of cardiovascular disease in hypertension.	American Journal of Hypertension	23	290-298	2010
Kawano Y.	Physio-pathological effects of alcohol on the cardiovascular system: its role in hypertension and cardiovascular disease.	Hypertension Research	33	181-191	2010
Horio T, Kamide K, Takiuchi S, Yoshii M, Miwa Y, Matayoshi T, Yoshihara F, Nakamura S, Tokudome T, Miyata T, Kawano Y.	Association of insulin-like growth factor-1 receptor gene polymorphisms with left ventricular mass and geometry in essential hypertension	Journal of Human Hypertension	24	320-326	2010

Authors	Title	Journal	Vol	Pages	Year
Kawano Y, Horio T, Kamide K, Iwashima Y, Yoshihara F, Nakamura S.	Blood pressure and medication during long-term antihypertensive therapy based on morning home systolic blood pressure in hypertensive patients: HOSP (Hypertension Control Based On Home Systolic Pressure) substudy.	Clinical and Experimental Hypertension	32	239-243	2010
*Horio T, Iwashima Y, Kamide K, Tokudome T, Yoshihara F, Nakamura S, Kawano Y.	Chronic kidney disease as an independent risk factor for new onset atrial fibrillation in hypertensive patients.	Journal of Hypertension	28	1738-1744	2010
Yamashita S, Bujo H, Arai H, Harada-Shiba M, Matsui S, Fukushima M, Saito Y, Kita T, Matsuzawa Y.	Long-Term Probucol Treatment Prevents Secondary Cardiovascular Events: a Cohort Study of Patients with Heterozygous Familial Hypercholesterolemia in Japan.	J Atheroscler Thromb.	15	292-303	2008
*Shimano H, Arai H, Harada-Shiba M, Ueshima H, Ohta T, Yamashita S, Gotoda T, Kiyohara Y, Hayashi T, Kobayashi J, Shimamoto K, Bujo H, Ishibashi S, Shirai K, Oikawa S, Saito Y, Yamada N.	Proposed Guidelines for Hypertriglyceridemia in Japan with Non-HDL Cholesterol as the Second Target.	J Atheroscler Thromb.	15	116-121	2008
Harada K, Miyamoto Y, Morisaki H, Ohta N, Yamanaka I, Kokubo Y, Makino H, Harada-Shiba M, Okayama A, Tomoike H, Okumura T, Saito Y, Yoshimasa Y, Morisaki T.	A novel Thr56Met mutation of the autosomal recessive hypercholesterolemia gene associated with hypercholesterolemia.	J Atheroscler Thromb.		in press	2010
Kang J, Tachibana Y, Kanata W, Mahara A, Harada-Shiba M, Yamaoka T.	Liver-targeted siRNA delivery by polyethylenimine(PEI)-pullulan carrir.	Bioorganic & Medicinal Chemistry	18	3946-3950	2010
Fujita Y, Kakino A, Harada-Shiba M, Sato Y, Otsui K, Yoshimoto R, Sawamura T.	C-Reactive Protein Uptake by Macrophage Cell Line via Class-A Scavenger Receptor.	Clinical Chemistry	56(3)	478-481	2010

著者	題名	雑誌名	巻(号)	頁	年
*Harada-Shiba M, Sugisawa T, Makino H, Abe M, Tsushima M, Yoshimasa Y, Yamashita T, Miyamoto Y, Yamamoto A, Tomoike H, Yokoyama S.	Impact of statin treatment on the clinical fate of heterozygous familial hypercholesterolemia.	Journal of Atherosclerosis and Thrombosis	17(7)	667-674	2010
斯波真理子	家族性高コレステロール血症 (FH)	循環器病研究の進歩（通巻50号）	31(1)	25-33	2010
山本剛史, 斯波真理子	LDL受容体のあらたな制御機構と治療戦略	医学のあゆみ	234 (7.8)	754-757	2010
斯波真理子, 山下貴裕	ARHとPCSK9	Medical Practice	27(3)	494-495	2010
斯波真理子, 山下貴裕	家族性高コレステロール血症の治療	Medical Practice	27(3)	527-532	2010
*Watanabe Y, Uotani K, Nakazawa T, Higashi M, Yamada N, Hori Y, Kanzaki S, Fukuda T, Itoh T, Naito H.	Dual-energy direct bone removal CT angiography for evaluation of intracranial aneurysm or stenosis: comparison with conventional digital subtraction angiography.	Eur Radiol.			2008 Nov 11
*Takigawa M, Akutsu K, Kasai S, Tamori Y, Yoshimuta T, Higashi M, Takeshita S.	Angiographic documentation of aortoiliac occlusion in Leriche's syndrome.	Can J Cardio.	24(7)	568	2008 Jul
*Kamiya C, Sakamoto S, Tamori Y, Yoshimuta T, Higashi M, Tanaka R, Akutsu K, Takeshita S.	Long-term outcome after percutaneous peripheral intervention vs medical treatment for patients with superficial femoral artery occlusive disease.	Circ J.	72(5)	734-739	2008 May
東 将浩	dual source CTを用いた冠動脈CT angiography	臨床画像	24(11)	46-54	2008
中沢一雄, 原口 亮, 東 将浩	代表的心疾患の最新画像診断, 心血管系の構造　心血管疾患診療のエクセレンス	日医雑誌	137	S2-3	2008

著者	題名	雑誌名	巻(号)	頁	年
東 将浩, 堀 祐郎, 中澤哲郎, 神崎 歩, 福田哲也, 山田直明, 魚谷健祐, 木曽啓祐, 内藤博昭, 圷 宏一	Dual Source CTを用いた冠動脈CTA	臨床放射線	54(1)	163-169	2009
宮田茂樹, 宮田敏行, 嘉田晃子, 長束一行	アスピリンレジスタンス	Brain and Nerve	60(11)	1365-1371	2008
宮田茂樹, 角谷勇実, 嘉田晃子	ヘパリン起因性血小板減少症(HIT)における血清学的診断の重要性とその問題点	日本検査血液学会雑誌	9(3)	409-418	2008

＊印のついている論文のみ別刷を添付

Ⅳ. 研究成果の刊行物・別刷
（抜粋）

診療

Dual source CT を用いた冠動脈 CTA

東　将浩[*1]　堀　祐郎[*1]　中澤哲郎[*1]　神崎　歩[*1]　福田哲也[*1]
山田直明[*1]　魚谷健祐[*1,3]　木曽啓祐[*1]　内藤博昭[*1]　圷　宏一[*2,4]

■ はじめに

マルチスライス CT の列数の増加，ガントリー回転速度の高速化により，心電図同期 CT が，簡便に行えるようになった[1]。特に，64 列マルチスライス CT の登場により，冠動脈 CT の検査数が飛躍的に増加し，診療報酬においても，冠動脈 CT 加算が算定できるようになった。

しかし，冠動脈 CT は，すべての患者において良好な画像が得られるのではなく，撮影時の注意や，撮影後の処理も必要である。また，高心拍[2]や不整脈患者，石灰化やステント留置例など解決すべき問題も多い。

二管球搭載型マルチスライス CT（dual-source CT, DSCT）は，1 台の CT 装置に，2 組の管球—検出器システムが直交した状態で搭載されている（図1）。管球回転時間は 330 ミリ秒であり，心電図同期撮影の際の時間分解能は，患者の心拍数にかかわらず 83 ミリ秒となる[3]。この優れた時間分解能により，高心拍数患者においても，心拍をコントロールすることなく，冠動脈 CT が実施可能と報告されている[1]。本研究の目的は，DSCT を用いた冠動脈 CT を心臓カテーテル検査による冠動脈造影と比較し，冠動脈描出能の評価，冠動脈狭窄病変に対する診断能を評価することにある。

❶ 対象と方法

2007 年 9 月〜 2008 年 3 月の間に，大動脈瘤の術前検査として胸腹部 CT と冠動脈造影が予定されている症例のうち，研究に対して文章による同意が得られた連続 48 症例を対象とした（男性 36 例，女性 12 例，平均年齢 70 歳）。平均体重 61kg（35 〜 86kg）。
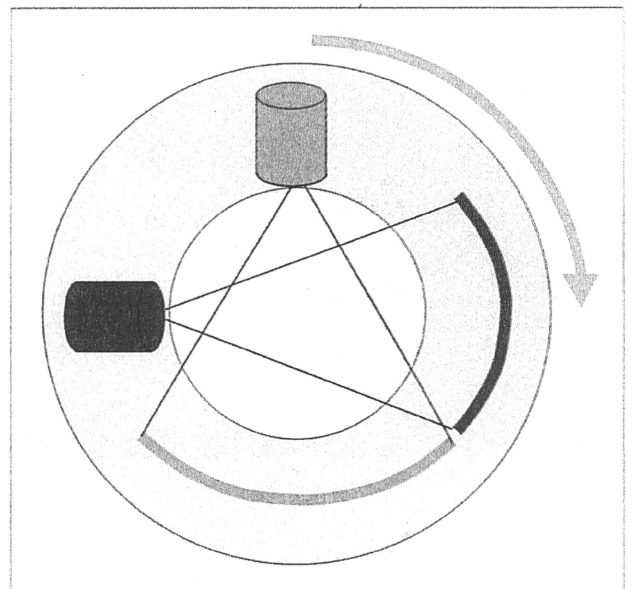
図1　DSCT のシェーマ
DSCT には X 線管と検出器のシステムが二組，お互いが直交する形で搭載されている。X 線管は同じだが，検出器の角度が異なる。

[*1]　M. Higashi, Y. Hori, T. Nakazawa, S. Kanzaki, T. Fukuda, N. Yamada, K. Uotani, K. Kiso, H. Naito　国立循環器病センター　放射線診療部　[*2]　K. Akutsu　同　心臓血管内科　[*3]　現　神戸大学医学部放射線科　[*4]　現　日本医科大学千葉北総合病院集中治療室
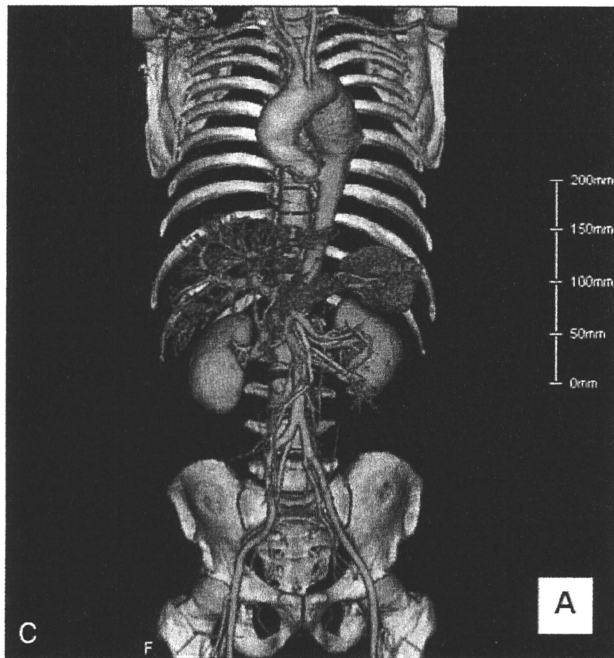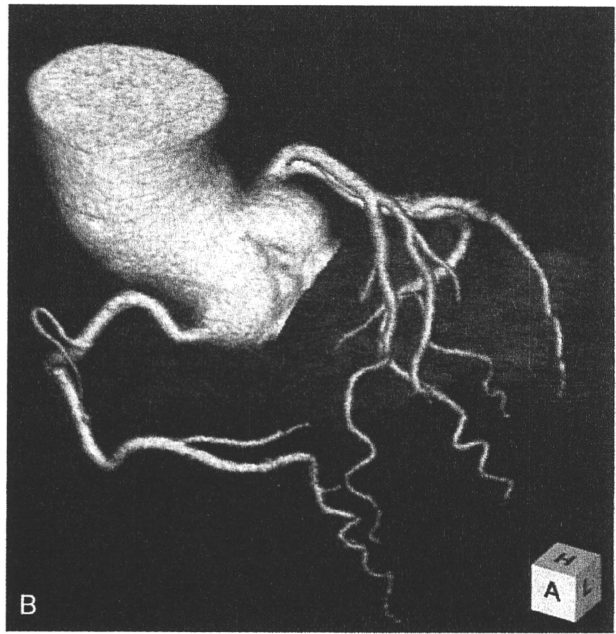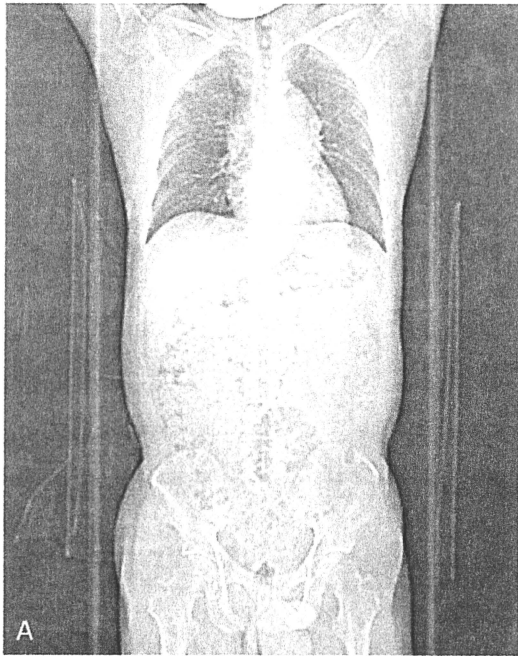〔索引用語：Dual source CT を用いた冠動脈 CT〕

図2　冠動脈＋胸腹部 CT にて得られた冠動脈と胸腹部の三次元画像（volume rendering）
造影早期相の始めに，冠動脈用に心電図同期で撮影。その直後に，胸腹部を非同期で撮影した。

緊急症例，ヨード造影剤に対するアレルギー，透析のされていない中等度以上の腎機能障害例，冠動脈バイパス術が施行されている例，心房細動症例は除外した。冠動脈 CT にて正常冠動脈と判断された例は，冠動脈造影を行わない条件下にて。本研究は倫理委員会の承認を得た。

使用した CT 装置は，2 管球搭載型 64 スライス CT（SOMATOM Definition, Siemens）。冠 動

脈 CT を造影早期相の胸腹部 CT の撮影前に行い，1 回の CT 検査，1 回の造影剤注入にて，冠動脈 CT，胸腹部 CT を撮影した（図 2）。冠動脈 CT の撮影範囲は，冠動脈が描出される最も頭側のスライスの 2cm 頭側から，心臓が含まれる最も尾側のスライスの 2cm 足側までとした。検出器は 32×0.6mm，x-flying focal spot によりスライス収集は 64×0.6mm となる。ガントリーの回転時間は 0.33 秒。管電圧

表1　本研究における冠動脈＋胸腹部 CT の造影プロトコール

```
造影剤 Iohexol 350mgI/ml or Iopamidol 370mgI/ml
二相注入：（注入速度）x（注入時間）
  第一相：(0.06ml/kg・sec) x（冠動脈 CT 撮影時間＋6 秒）
        （注入速度：min 3ml/sec, max 5ml/sec）
  第二相：(0.03ml/kg・sec) x（胸腹部 CT 撮影時間＋5 秒）
        （注入速度：min 1.5ml/sec, max 2.5ml/sec）
  後押し用生理食塩水 0.03ml/kg, sec 25ml
bolus tracking 法：上行大動脈 CT 値 > 単純 CT ＋100H.U.
ベータ遮断薬の投与なし
ミオコールスプレー舌下投与
```

は 120kV，管電流は 380mAs/rotation。ビームピッチは患者心拍数に依存した可変式であり，高心拍数では大きくなる（0.2 ～ 0.5）。全例，ニトログリセリンの舌下投与を行った。CT 撮影のための β 遮断薬は使用しなかった。

表1に本研究における造影剤の使用法を示す。造影剤は，イオパミドール 370mgI/ml またはイオヘキソール 350mgI/ml を使用し，二相注入と生理食塩水による後押しをした。一相目の注入速度は，0.06ml/kg・sec（最低 3ml/sec，最高 5ml/sec），注入時間は，冠動脈 CT の撮影時間に 6 秒を加えた時間とした。二相目の注入速度は，0.03ml/kg・sec（最低 1.5ml/sec，最高 2.5ml/sec），つまり第一相の半分の注入速度，注入時間は，胸腹部 CT の撮影時間に 5 秒を加えた時間とした。

撮影開始のタイミングは bolus tracking 法により決定した。上行大動脈に関心領域を設定し，閾値は，単純 CT プラス 100H.U. 以上とした。

画像再構成は，FOV = 20cm，スライス厚 = 0.6mm，再構成間隔 = 0.3mm，再構成関数 = B26f で行った。再構成心時相の決定には，まず，本体に搭載されている最適拡張期，最適収縮期を抽出する機能を使用した。アーチファクトにより，三次元画像処理に適さないと判断した場合には，マニュアルにて，最適心時相を探索した。

ワークステーション（ZIOSTATION，ZIOSOFT）上で，MIP，CPR を作成した。内径 1.5mm 以上の冠動脈に対して，AHA 分類によるセグメントごとに，有意狭窄の有無が判断可能かどうかを判定した。冠動脈造影が行われた症例に対しては，50%を超える狭窄の有無を判定し，冠動脈造影の結果と比較した。

❷ 結　果

全症例で検査を施行できた。撮影時の平均心拍数は，毎分 64 回（43 ～ 107 回）。冠動脈 CT の撮影時間は，平均 9.1 秒（4.7 ～ 13.4 秒）。使用造影剤は，平均 91ml（66 ～ 144ml）となった。

607 セグメント中 571 セグメントで評価可能であった。評価不能は 36 セグメント（5.9%）であった。評価不能の原因は，モーションアーチファクトが 22 セグメント，石灰化が 5 セグメント，ステントが 9 セグメントであった。

13 症例において，冠動脈 CT にて正常冠動脈と診断し，冠動脈造影は行わなかった（図3）。35 例にて冠動脈造影と比較した。409 セグメント中 391 セグメントにおいて，狭窄の有無が一致した（図4, 5）。感度 86%，特異度 97%，正診率 96%，陽性予測率（positive predictive value，PPV）76%，陰性予測率（negative predictive value，NPV）98%となった（表2）。

表2　結果

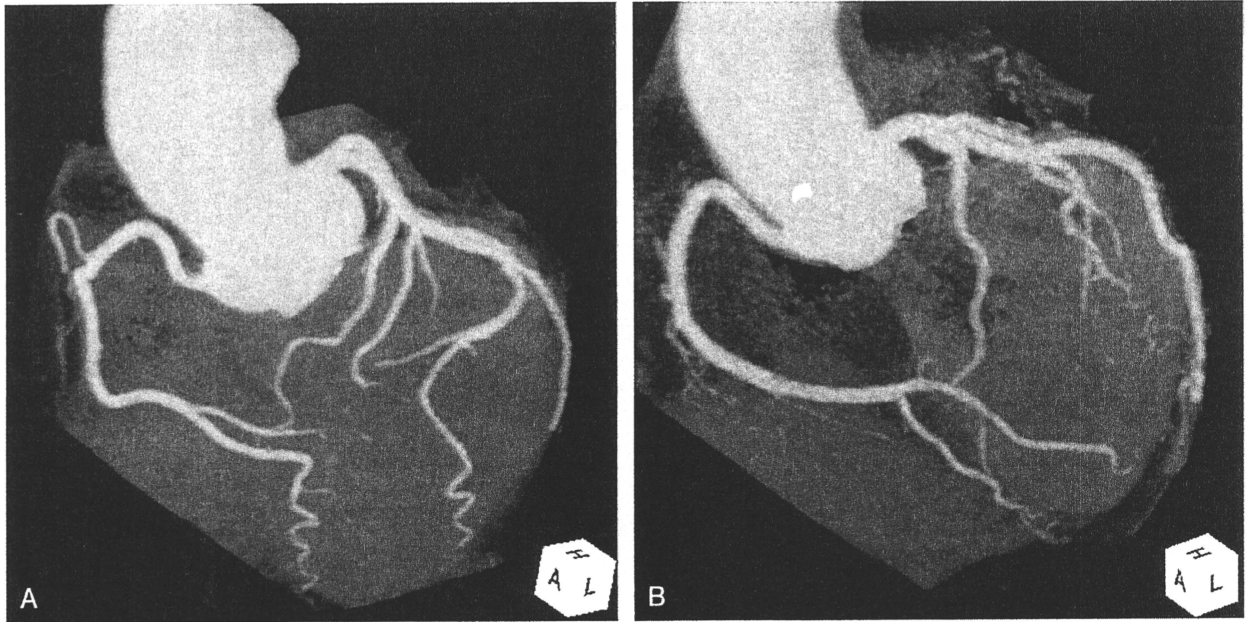| CT	CAG	
	なし	あり
なし	354	6
あり	12	37

感度＝ 86%，特異度＝ 97%，正診率＝ 96%
陽性予測率＝ 76%，陰性予測率＝ 98%

図3 冠動脈 CT, MIP 像
A, B 冠動脈 CT にて, 正常冠動脈と判断され, 冠動脈造影が省略された例。平均心拍数 46 回 / 分。

❸ 考　察

　マルチスライス CT を用いた冠動脈 CT は, 4 列の時代から報告されている。その当時から, 高い特異度, 陰性予測率（NPV）を示していた。つまり, 有意狭窄のない冠動脈を有意狭窄なしと診断し, 冠動脈 CT で有意狭窄がない場合は, 実際に狭窄がない確率が非常に高い検査といえる。しかし, モーションアーチファクトや石灰化により診断できない領域が多いこと, 狭窄を過大評価し疑陽性が比較的多いことが問題と

してあげられていた（表3）。
　CT の進歩により, 時間分解能, 空間分解能が向上し, 撮影時間の短縮とあわせ, 診断可能領域の割合が増え, 感度も上昇してきている（表3）。しかし, 従来型のマルチスライス CT では, 時間分解能の制限により, 高心拍数の患者ではアーチファクトが多くなり, 診断能が低下する傾向にあった。そのため, ベータ遮断薬の使用や, ガントリーの回転時間を調整する必要があった。
　一方, DSCT においては, すべての心拍数に対し

表3　冠動脈 CT の描出能, 狭窄に対する診断能の報告

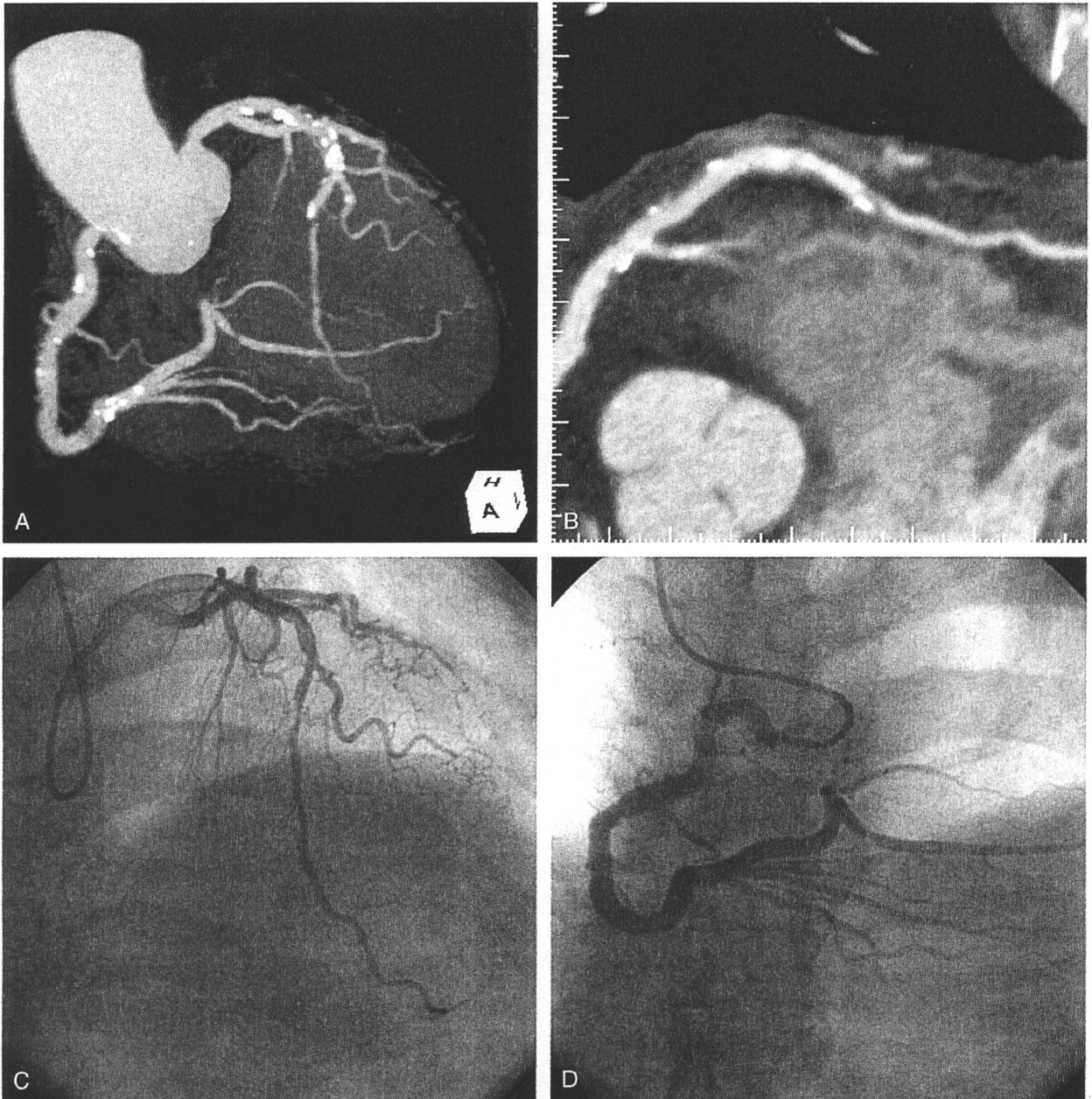|	対象血管	評価可能 (%)	狭窄度	感度 (%)	特異度 (%)	NPV (%)
Nieman et al[5]	4-MSCT	≧ 2.0mm	70	≧ 50%	82	93	97
Achenbach et al[6]	4-MSCT	≧ 2.0mm	68	≧ 70%	91	84	98
Nieman et al[7]	16-MSCT	≧ 2.0mm	93	> 50%	95	86	97
Achenbach et al[8]	16-MSCT	≧ 1.5mm	96	> 50%	94	96	99
Ropers et al[9]	64-MSCT	> 1.5mm	96	> 50%	93	97	100
Scheffel et al[4]	DSCT	> 1.5mm	98.6	> 50%	96.4	97.5	99.4
本研究	DSCT	≧ 1.5mm	94	> 50%	86	97	98

NPV：negative predictive value

図4　冠動脈 CT と冠動脈造影の対比，狭窄部の対比
A　MIP 像　B　CPR 像　C　左冠動脈造影　D　右冠動脈造影

て 83 ミリ秒という時間分解能を有するため，これら高心拍数の患者においても心拍数のコントロールなしに，冠動脈 CT が可能と報告されている[4]。今回の我々の検討においても，心拍数をコントロールすることなく，良好な画像を得ることができた。

　我々の施設では，大動脈瘤の術前検査として，胸腹部の造影 CT を行い，大動脈の三次元画像を作成している。一方，冠動脈造影は，胸部大動脈瘤では全例，腹部大動脈瘤では冠動脈疾患のリスクが高い症例に対して施行している。つまり，大動脈瘤の術前患者群は，CT と冠動脈造影の両方が行われる確率が高い患者群となる。胸腹部 CT に冠動脈 CT を組み込み 1 回の検査とすることで，検査に対する患者の負担を減らした研究を行った。本研究は，純
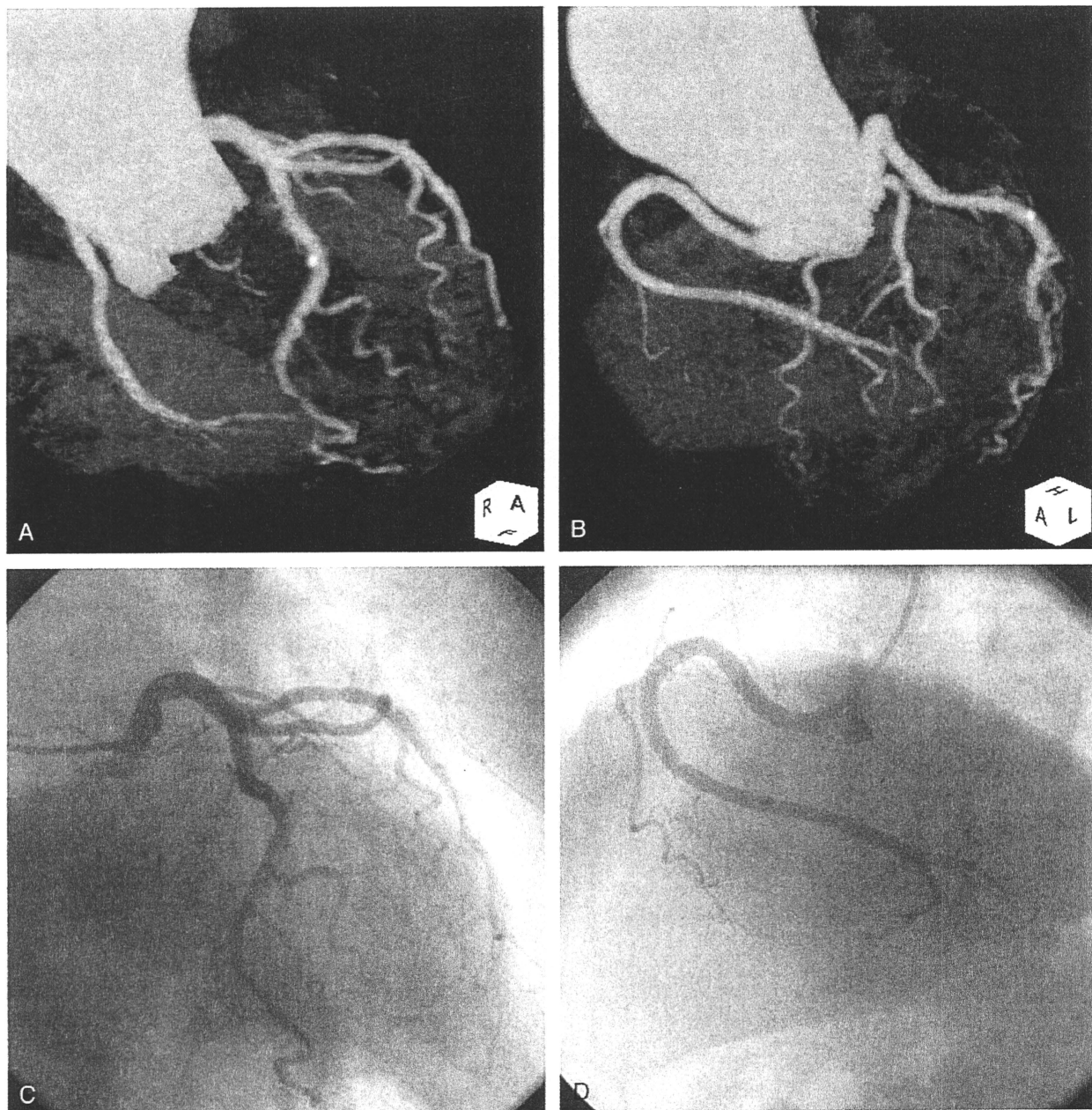
図 5　冠動脈 CT と冠動脈造影の対比, 高心拍数症例
A, B　MIP 像　C　左冠動脈造影　D　右冠動脈造影　撮影時の平均心拍. 毎分 107 回。

粋な冠動脈 CT のみの撮影ではないが, 造影早期
相の前半に冠動脈 CT 撮影しているため, 冠動脈
CT のみの場合でも, 同様の診断能が得られると期待
している。

　冠動脈 CT においては, 評価可能な領域を増やす
ためアーチファクトや石灰化を含む領域を無理に判定
すると, 正診率が低下する可能性がある。逆に, 正

診率を高いレベルに保とうとすると, 評価不能な領域
が増えるかもしれない。冠動脈 CT の特徴は, やはり
高い陰性予測率である。つまり, 冠動脈 CT で狭窄
がないと判断した場合, 狭窄のある可能性がきわめ
て低い。これを前提にしたうえで CT を利用する方が,
冠動脈 CT の特性を生かせると思われる。

　冠動脈 CT の適応に関しては, 症状を有する中等

168

度の pre-test probability 患者に対して有用性が高いとされている[16]。これは，危険因子が多い症例では，診断できない場合も多く，狭窄が疑われた場合にも，CT では完結せず冠動脈造影が実施される可能性が高いことによる。また危険因子が少ない症例では，被曝や造影剤の副作用（患者の不利益）と，狭窄が発見される（患者の利益）確率を考えた場合，患者利益の方が低いと考えられるからである。しかし，危険因子が低い症例は石灰化が少ない可能性が高く，CT で検査を完結できる可能性が高いと予想される。今回検討した患者群のように，冠動脈 CT により冠動脈造影が省略できるのであれば，冠動脈 CT の有用性は非常に高いと考える。

■ ま と め

DSCT を用いた冠動脈 CTA を行い，冠動脈造影との比較をした。β遮断薬を使用することのない条件下で，診断可能なセグメントが 94% であった。冠動脈狭窄に対する陰性予測率が高かった（98%）。

文　献 ·····················

1) Achenbach S : Computed tomography coronary angiography. J Am Coll Cardiol 48 : 1919-1928, 2006

2) Giesler T et al : Noninvasive visualization of coronary arteries using contrast-enhanced multidetector CT : in uence of heart rate on image quality and stenosis detection. AJR 179 : 911-916, 2002

3) Flohr T et al : First performance evaluation of a dual-source CT (DSCT) system. Eur Radiol 16 : 256-268, 2006

4) Scheffel H et al : Accuracy of dual-source CT coronary angiography : first experience in a high pre-test probability population without heart rate control. Eur Radiol 16 : 2739-2747, 2006

5) Nieman K et al : Usefulness of multislice computed tomography for detecting obstructive coronary artery disease. Am J Cardiol 89 : 913-918, 2002

6) Achenbach S et al : Detection of coronary artery stenoses by contrast-enhanced, retrospectively electrocardiographically-gated, multislice spiral computed tomography. Circulation 103 : 2535-2538, 2001

7) Nieman K et al : Reliable noninvasive coronary angiography with fast sub-millimeter multislice spiral computed tomography. Circulation 106 : 2051-2054, 2002

8) Achenbach S et al : Detection of coronary artery stenoses using multi-detector CT with 16 3 0.75 collimation and 375 ms rotation. European Heart Journal 26 : 1978-1986, 2005

9) Ropers D et al : Usefulness of multidetector row computed tomography with 64 0.6 mm collimation and 330-ms rotation for the noninvasive detection of signifcant coronary artery stenoses. Am J Cardiol 97 : 343-348, 2006

10) Robert C et al : Criteria for cardiac computed tomography and cardiac magnetic resonance imaging. JACC 48 : 1475-1497, 2006

Summary

Coronary CT angiography with dual-source CT

The purpose of this study was to assess the diagnostic accuracy of dual-source computed tomography (DSCT) for evaluation of coronary artery disease (CAD). DSCT has high temporal resolution (83msec in any RR interval). DSCT-CAG was performed in consecutive pre-operative 48 patients with aortic aneurysm or dissection. Assessable segments were 571 of 607 (94%). DSCT-CAG was compared with conventional CAG in 35 patients. Segment based sensitivity, specificity, positive and negative predictive value for evaluating CAD were 86%, 97%, 76%, and 98%, respectively.

Masahiro Higashi et al
Department of Radiology
National Cardiovascular Center

NEURO

Dual-energy direct bone removal CT angiography for evaluation of intracranial aneurysm or stenosis: comparison with conventional digital subtraction angiography

Yoshiyuki Watanabe
Kensuke Uotani
Tetsuro Nakazawa
Masahiro Higashi
Naoaki Yamada
Yoshiro Hori
Suzu Kanzaki
Tetsuya Fukuda
Toshihide Itoh
Hiroaki Naito

Y. Watanabe · K. Uotani ·
T. Nakazawa · M. Higashi ·
N. Yamada · Y. Hori · S. Kanzaki ·
T. Fukuda · H. Naito
Department of Radiology,
National Cardiovascular Center,
Osaka, Japan

Y. Watanabe (✉)
Department of Radiology,
St. Luke's International Hospital,
9-1 Akashicho, Chuo-ku,
Tokyo, 104-8565, Japan
e-mail: yowatana@luke.or.jp
Tel.: +81-6-68335012
Fax: +81-6-68727486

T. Itoh
Siemens Asahi Medical Technologies,
Tokyo, Japan

Abstract Dual energy CT can be applied to bone elimination for cerebral CT angiography (CTA). The aim of this study was to compare the results of dual energy direct bone removal CTA (DE-BR-CTA). To those of DSA. Twelve patients with intracranial aneurysms and/or ICA stenosis were performed on a dual-source CT in dual energy mode. A post-processing software selectively remove bone structures using the two energy data sets. 3D-images with and without bone removal were reviewed and compared to DSA. Dual energy bone removal was successful in all patients. For 10 patients, bone removal was good and CTA MIP images could be used for vessel evaluation. For 2 patients, bone removal was moderate with some bone remnants but this did not disturb the 3D visualization. Three aneurysms adjacent to the skull base were only partially visible in conventional CTA but were fully visible in DE-BR-CTA. In 5 patients with ICA stenosis, DE-BR-CTA revealed the stenotic lesions on the MIP images. The correlation between DSA and DE-BR-CTA was good ($R^2=0.822$), but DE-BR-CTA lead to an overestimation of stenosis. DE-BR-CTA is able to eliminate bone structure using only a single CT data acquisition and is useful to evaluate intracranial aneurysms and stenosis.

Keyword Cerebral CTA ·
Dual-energy CT · Dual-source CT ·
Bone elimination · Brain

Introduction

Cerebral computed tomography angiography (CTA) has become a powerful, noninvasive diagnostic tool for evaluating cerebrovascular disease [1–3]. However, single-source CTA still has drawbacks compared to digital subtraction angiography (DSA), in particular for the evaluation of arteries with calcified plaque or vessels located next to the skull bone, as these vasculatures cannot

be unambiguously distinguished from surrounding bony or calcified structures. This problem can be solved by applying subtracting CTA to a noncontrast and a contrast CT data set to eliminate bones [4–8]. Dual-source, dual-energy CT has the potential to distinguish iodine from bone or calcifications using the attenuation difference between the two energies [9].

Here, we evaluated the performance of dual-energy direct bone removal CTA (DE-BR-CTA) for diagnosing

brain aneurysms, internal carotid artery (ICA) stenosis, or both. We also compared the DE-BR-CTA findings with those of DSA.

Materials and methods

Subjects

This study was performed after obtaining approval of the local institutional review board. Written informed consent was obtained from all patients. We prospectively selected 12 patients (7 male, 5 female; 36–78 years, mean 64 years) who underwent both DE-BR-CTA and DSA within 30 days of each other. Nine patients were suspected of intracranial unruptured aneurysms with MR angiography. Five patients were suspected of ICA stenosis. Of these five, three patients had a stroke and in two patients the asymptomatic stenosis was found during the evaluation for aneurysm.

CTA protocol

CTA was performed using a dual-source CT system (SOMATOM Definition, Siemens, Germany). CT parameters in the dual-energy mode were 140 and 80 kV tube voltage, 80 and 360 effective mAs, respectively. 0.5-s rotation time, 64×0.6-mm collimation with z-flying focal spot, and a pitch of 0.6. The 140 and 80 kV images (dual-energy images) were reconstructed separately in sections that were 0.75 mm wide at 0.5 mm increments using a D30 kernel for a field of view of 180 mm. Contrast material (350 mg I/ml) was injected for 20 s via the antecubital vein, followed by a 25 ml saline flush. Injection rate and dose depended on the patient's weight: 3.0 ml/s, 60 cc for patients weighing less than 60 kg; 3.5 ml/s, 70 cc for patients weighing less than 70 kg; and 4 ml/s, 80 cc for those over 70 kg. The delay time of the CT data acquisition after the injection was determined using a bolus tracking software at the basilar artery or ICA.

DSA was performed using a biplane DSA unit with rotational 3D DSA (INTEGRIS BV3000, Philips Healthcare, Best, Netherland).

Image processing and analysis

The dual-energy images were transferred to a workstation (Multi Modality Workplace; Siemens Medical Solutions, Germany), and the prototype of a commercial software (Syngo 2008G) was used to create a DE-BR-CTA from which the bone voxels had been removed ("head bone removal" application). The combined images of both energy data were reconstructed and used for diagnostic reading (conventional CTA).

Fig. 1 Right ICA large aneurysm of a 75-year-old female patient. MIP images of DE-BR-CTA (a, c) delineate the general shape and configuration of aneurysm as well as DSA (d). VR image of conventional CTA (b) did not show the caudal side of aneurysm with bone
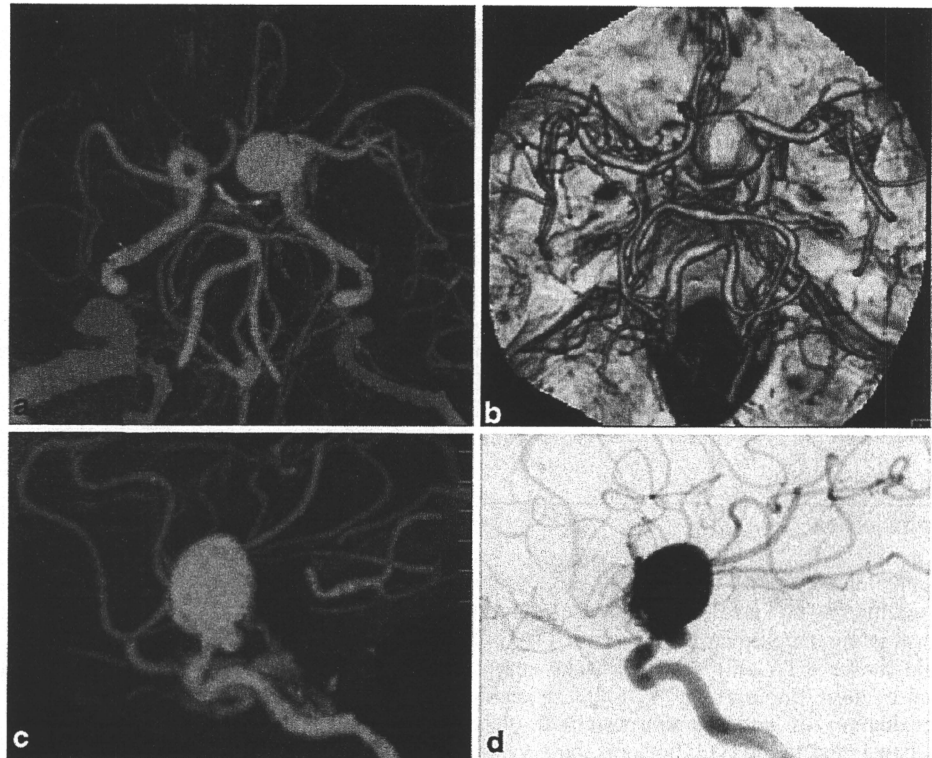
Fig. 2 Left MCA calcified aneurysm and bilateral ICA stenosis with hard plaque in a 77-year-old female patient. MIP image of DE-BR-CTA (a) removed the calcifications of ICA and aneurysm and revealed the same aneurysm shape as with DSA (b). However, the DE-BR-CTA (a) shows a short defect at the severe stenotic site at ICA terminal (arrow). CTA source images (c) show dense calcifications around the whole circumference of the ICA and anterior wall of the left MCA aneurysm (arrowheads). VR image of conventional CTA (d) showed the dense calcification at bilateral ICA and aneurysms, but failed to reveal details
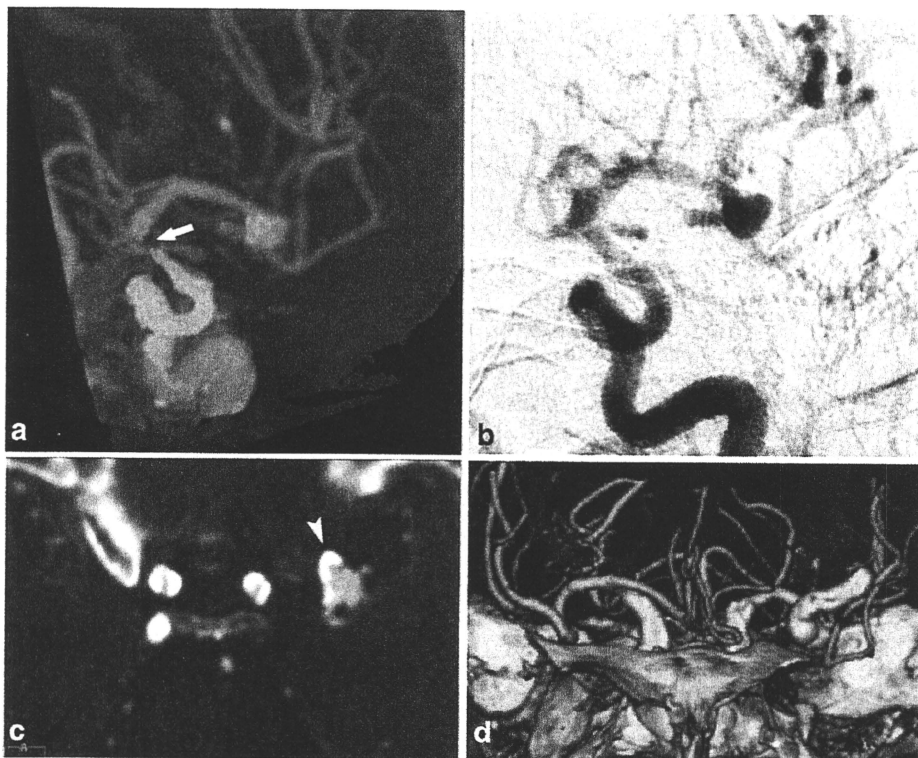
Two neuroradiologists blinded to all clinical information independently reviewed the DE-BR-CTA in maximum-intensity projection (MIP) and the conventional CTA in volume-rendering (VR) technique on a 3D workstation. Disagreements regarding final conclusions were resolved by consensus.

The quality of the dual-energy bone removal was rated according to a four-point scale. "Excellent" was defined as clearly visible vasculature and no bone remnants, "good" as discernable vasculature and containing only tiny bone remnants, "moderate" as containing larger bone remnants that did not however disturb the vessel visualization, and
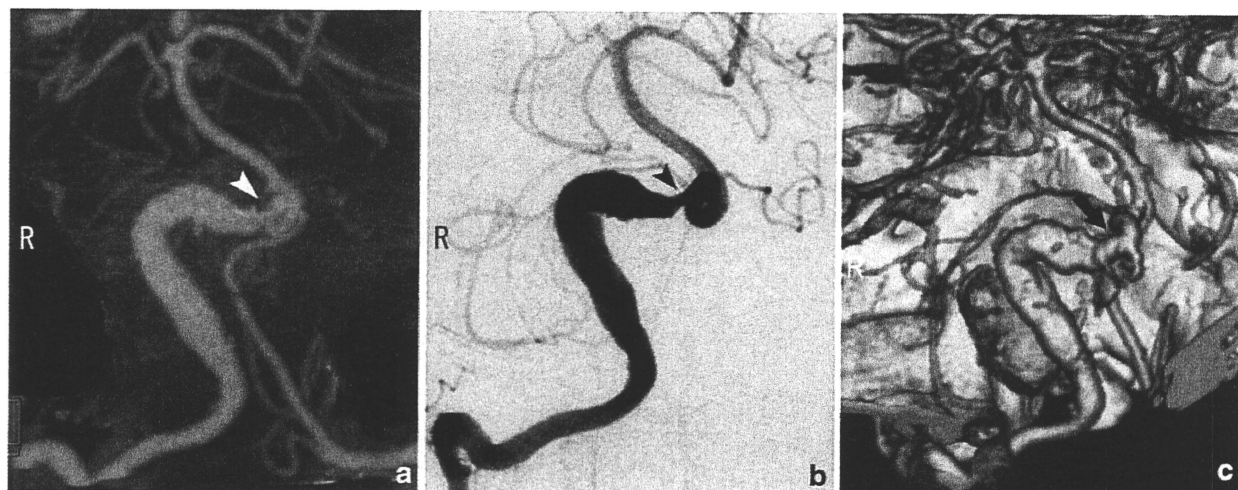
Fig. 3 Right vertebral artery fusiform aneurysm with calcification in a 55-year-old male patient. MIP image of DE-BR-CTA (a) removed the calcification of aneurysm and revealed the distal-end stenosis (arrowhead) of the aneurysm as with DSA (b). VR image of conventional CTA (c) showed the calcification (arrow), but the stenosis is hard to see

"poor" as including large bone remnants or artifacts covering parts of the vessels.

Further, the visibility of the ophthalmic artery in DE-BR-CTA was rated according to a four-point scale. "Excellent" was defined as the ophthalmic artery being visible from the origin to the intra-orbital portion, "good" as one artery being visible and the other with only the origin or other short segments being detected, "poor" as the long segment of the ophthalmic artery being detected, and "not visible" as the ophthalmic artery not being discernable at all.

For the evaluation of aneurysm, conventional CTA and DE-BR-CTA were compared for the detection and delineation of aneurysms and compared to the DSA results.

For the evaluation of ICA stenosis, the DE-BR-CTA and DSA were compared and the degree of stenosis was calculated using the Warfarin-Aspirin Symptomatic Intracranial Disease Study method [10], which is the ratio of the diameter of the maximum stenotic site to the diameter of the proximal normal ICA.

Kappa statistics were used to assess interobserver reliability. Kappa values above 0 were considered to indicate positive agreement: less than 0.4, positive but poor agreement; 0.41–0.75, good agreement; and more than 0.75, excellent agreement.

Results

Dual-energy bone removal was successful in all patients and the post-processing of DE-BR-CTA took an average of 53 s, excluding data transfer and saving time. The quality
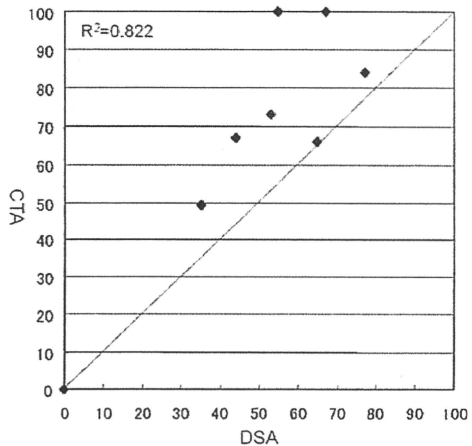

Fig. 5 Scatterplots illustrate percentages of carotid artery stenosis at DE-BR-CTA versus DSA. Good correlation was noted between the two methods ($R^2 = 0.822$), but the stenosis diagnosed by CTA was higher than that by DSA for most cases

of dual-energy bone removal was rated "excellent" for two of the patients, "good" for eight patients, and "moderate" for two patients.

Of the 24 ophthalmic arteries, the visibility of 7 was rated "excellent," 14 were rated "good," 1 was rated "poor," and 2 arteries were rated "not visible." The two ophthalmic arteries that were not visible in DE-BR-CTA were found by DSA to be occluded. Interobserver reliability between two readers was good for quality of bone removal (k=0.60) and visibility of ophthalmic arteries (k=0.65).

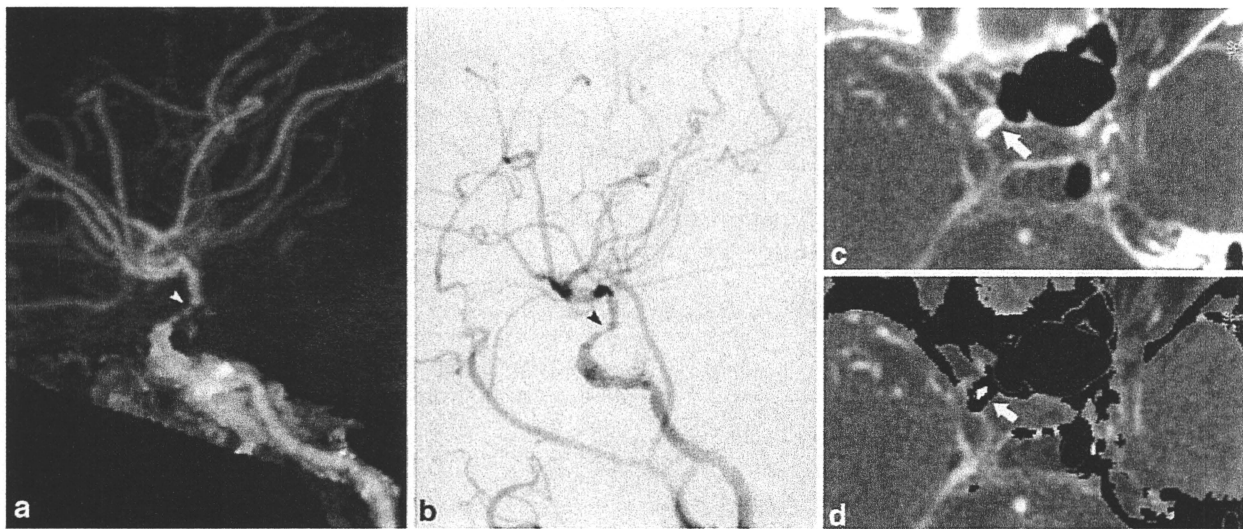Aneurysms were located in the vertebral artery (two patients), basilar artery (one patient), ICA (two patients),

Fig. 4 Right ICA severe stenosis of a 67-year-old female patient. C2 portion of ICA had severe stenosis (*arrowhead*) demonstrated by DE-BR-CTA (**a**) and DSA (**b**). The ophthalmic artery is not visualized by DE-BR-CTA or by DSA. CTA source images (**c**) show dense calcifications around the whole circumference of the right ICA, and these calcifications were removed after DE bone-removal post-processing (**d**)

middle cerebral artery (MCA: three patients) and anterior communicating artery (ACOM: one patient).

Three aneurysms (two ICA and one MCA) adjacent to the skull base were only partially visible in conventional CTA but were fully visible in DE-BR-CTA (Fig. 1). For three aneurysms with calcifications [two MCA and one vertebral artery (VA)], the calcifications were removed by the head bone removal applications, and the intraluminal shape of the aneurysms was visualized precisely with results confirmed by DSA (Figs. 2, 3).

In five patients with ICA stenosis by calcification at the intercavernous or paraclinoid portion, the eight stenotic lesions were not visible in conventional CTA. However, after bone removal post-processing with dual energy, all stenotic lesions became clearly visible on the MIP images (Figs. 2, 4). The agreement of percent stenosis for the two methods is represented in the scatterplots shown in Fig. 5. The correlation between DSA and CTA was good (R^2= 0.822), and the majority of discordant points were above the line of correlation, indicating an overestimation of stenosis found on DE-BR-CTA compared to DSA.

Discussion

Our study shows that bone removal brain CTA using dual-energy data was useful to evaluate aneurysms and ICA stenosis with a short calculating time, and the results with DE-BR-CTA were comparable to those with DSA.

Dual-energy CT was developed during the late 1970s for tissue characterization using single-source, single-slice CT [11, 12] and mainly applied for bone densitometries [13, 14]. However, the limitation of CT hardware and software technology hampered expansion to further clinical applications [15].

Dual-source CT with dual-energy mode can acquire two different energy data into a single acquisition. Dual-energy CT imaging makes it possible to differentiate between certain materials, since X-ray absorption is material specific and dependent on the energy of the X-rays. Dual-energy CT for tissue characterization was reported for urinary stone differentiation [16–18], visualization of the knee ligament [19], and differentiation of iodine from bone and calcification [9].

Multi-slice CTA has a high sensitivity and specificity for the detection of intracranial aneurysm [1, 20].

Subtraction methods for bone removal in cerebral CTA have been reported for the evaluation of skull base aneurysm or extracranial ICA, such as simple subtraction from enhanced data to noncontrast data [4, 21]. More recently, selective bone removal or "matched mask bone elimination" have been widely used for bone-subtraction CTA where the bone mask image as well as the 3D registration to the enhanced CT acquisition were determined by a low-dose unenhanced CT acquisition [6–8].

In our study, DE-BR-CTA removed the bone structures very well, and the three aneurysms adjacent to the skull base were fully visible from all directions, in contrast to the partial view in conventional CTA.

Calcification of the aneurysmal wall makes surgical clipping difficult, so this information was important for deciding treatment strategies [22]. Conventional CTA images revealed calcifications but neither VR nor MIP images allowed a precise evaluation of the intraluminal aneurysmal shape. By comparison, the geometry of intraluminal aneurysms was clearly visible on DSA, yet calcifications could not be displayed. We found that calcifications of three aneurysms were removed by dual-energy bone removal, therefore the wall and luminal information of the aneurysms could be analyzed with both DE-BR-CTA and conventional CTA.

The advantage of the dual-energy bone removal method compared to CT digital subtraction methods is that it avoids the additional preliminary unenhanced CT acquisition. Single data acquisition reduces the radiation dose to the patient and also shows no misregistration artifacts. Subtraction methods use position adjustment, but if a patient moves between the two consecutive acquisitions, it becomes difficult to achieve a perfect match between the two images.

For the evaluation of intracranial stenosis and occlusion, DSA has been considered the reference standard [10]. The correlation between degree of intracranial stenosis based on CTA and DSA was excellent [23], and CTA has a higher sensitivity and positive predictive value than MRA [24]. Evaluation of ICA stenosis at the petrosal portion of carotid siphon or in cases of calcified plaque has not been reported previously, because CTA did not allow 3D visualization of ICA with these conditions. In contrast, DE-BR-CTA removed bone and calcifications and was able to measure the degree of stenosis.

As described above, we quantitatively evaluated ICA stenosis on MIP image. The correlation coefficient between DE-BR-CTA and DSA results was good, but stenosis tends to be overestimated in DE-BR-CTA compared to DSA. In our study, two severe stenotic arteries were misclassified as occluded (100% stenosis) with DE-BR-CTA. The main reason for this overestimation is blooming effects from calcifications. The poor enhancement of an artery with severe stenosis compared to a nonstenotic artery also makes it difficult to draw a clear demarcation between calcification and iodine. This problem might be resolved by optimization of demarcation parameters and reconstruction kernel.

Conclusion

Dual-energy bone removal using dual-source CT is able to eliminate bone and calcification from CTA images using only a single contrast-enhanced scan. DE-BR-CTA is a useful tool to evaluate intracranial aneurysms and stenosis.

1024

References

1. Agid R, Lee SK, Willinsky RA et al (2006) Acute subarachnoid hemorrhage: using 64-slice multidetector CT angiography to "triage" patients' treatment. Neuroradiology 48(11):787–794
2. Hashimoto H, Iida J, Hironaka Y et al (2000) Use of spiral computerized tomography angiography in patients with subarachnoid hemorrhage in whom subtraction angiography did not reveal cerebral aneurysms. J Neurosurg 92(2):278–283
3. Hirai T, Korogi Y, Ono K et al (2001) Preoperative evaluation of intracranial aneurysms: usefulness of intraarterial 3D CT angiography and conventional angiography with a combined unit–initial experience. Radiology 220(2):499–505
4. Jayakrishnan VK, White PM, Aitken D et al (2003) Subtraction helical CT angiography of intra- and extracranial vessels: technical considerations and preliminary experience. AJNR Am J Neuroradiol 24(3):451–455
5. Lell M, Anders K, Klotz E et al (2006) Clinical evaluation of bone-subtraction CT angiography (BSCTA) in head and neck imaging. Eur Radiol 16(4):889–897
6. Sakamoto S, Kiura Y, Shibukawa M et al (2006) Subtracted 3D CT angiography for evaluation of internal carotid artery aneurysms: comparison with conventional digital subtraction angiography. AJNR Am J Neuroradiol 27(6):1332–1337
7. Tomandl BF, Hammen T, Klotz E et al (2006) Bone-subtraction CT angiography for the evaluation of intracranial aneurysms. AJNR Am J Neuroradiol 27(1):55–59
8. Venema HW, Hulsmans FJ, den Heeten GJ (2001) CT angiography of the circle of Willis and intracranial internal carotid arteries: maximum intensity projection with matched mask bone elimination-feasibility study. Radiology 218(3):893–898
9. Johnson TR, Krauss B, Sedlmair M et al (2007) Material differentiation by dual energy CT: initial experience. Eur Radiol 17(6):1510–1517
10. Samuels OB, Joseph GJ, Lynn MJ et al (2000) A standardized method for measuring intracranial arterial stenosis. AJNR Am J Neuroradiol 21(4):643–646
11. Chiro GD, Brooks RA, Kessler RM et al (1979) Tissue signatures with dual-energy computed tomography. Radiology 131(2):521–523
12. Millner MR, McDavid WD, Waggener RG et al (1979) Extraction of information from CT scans at different energies. Med Phys 6(1):70–71
13. Genant HK, Boyd D (1977) Quantitative bone mineral analysis using dual energy computed tomography. Invest Radiol 12(6):545–551
14. Laval-Jeantet AM, Cann CE, Roger B et al (1984) A postprocessing dual energy technique for vertebral CT densitometry. J Comput Assist Tomogr 8(6):1164–1167
15. Kelcz F, Joseph PM, Hilal SK (1979) Noise considerations in dual energy CT scanning. Med Phys 6(5):418–425
16. Primak AN, Fletcher JG, Vrtiska TJ et al (2007) Noninvasive differentiation of uric acid versus non-uric acid kidney stones using dual-energy CT. Acad Radiol 14(12):1441–1447
17. Scheffel H, Stolzmann P, Frauenfelder T et al (2007) Dual-energy contrast-enhanced computed tomography for the detection of urinary stone disease. Invest Radiol 42(12):823–829
18. Graser A, Johnson TR, Bader M et al (2008) Dual energy CT characterization of urinary calculi: initial in vitro and clinical experience. Invest Radiol 43(2):112–119
19. Sun C, Miao F, Wang XM et al (2008) An initial qualitative study of dual-energy CT in the knee ligaments. Surg Radiol Anat 30(5):443–447
20. Pozzi-Mucelli F, Bruni S, Doddi M et al (2007) Detection of intracranial aneurysms with 64 channel multidetector row computed tomography: comparison with digital subtraction angiography. Eur J Radiol 64(1):15–26
21. Gorzer H, Heimberger K, Schindler E (1994) Spiral CT angiography with digital subtraction of extra- and intracranial vessels. J Comput Assist Tomogr 18(5):839–841
22. Hoit DA, Malek AM (2006) Fusion of three-dimensional calcium rendering with rotational angiography to guide the treatment of a giant intracranial aneurysm: technical case report. Neurosurgery 58(1 Suppl):173–174
23. Nguyen-Huynh MN, Wintermark M, English J et al (2008) How accurate is CT angiography in evaluating intracranial atherosclerotic disease? Stroke 39(4):1184–1188
24. Bash S, Villablanca JP, Jahan R et al (2005) Intracranial vascular stenosis and occlusive disease: evaluation with CT angiography, MR angiography, and digital subtraction angiography. AJNR Am J Neuroradiol 26(5):1012–1021

Kensuke Uotani
Yoshiyuki Watanabe
Masahiro Higashi
Tetsuro Nakazawa
Atsushi K. Kono
Yoshiro Hori
Tetsuya Fukuda
Suzu Kanzaki
Naoaki Yamada
Toshihide Itoh
Kazuro Sugimura
Hiroaki Naito

Dual-energy CT head bone and hard plaque removal for quantification of calcified carotid stenosis: utility and comparison with digital subtraction angiography

K. Uotani (✉)
7-5-2 Kusuhoki-cho, Chuo-ku, Kobe,
Hyogo, 650-0017, Japan
e-mail: uota2@med.kobe-u.ac.jp
Tel.: +81-78-382-6104
Fax: +81-78-382-6129

K. Uotani · Y. Watanabe · M. Higashi ·
T. Nakazawa · A. K. Kono · Y. Hori ·
T. Fukuda · S. Kanzaki · N. Yamada ·
H. Naito
Department of Radiology,
National Cardiovascular Center,
Suita, Osaka, Japan

K. Uotani · K. Sugimura
Department of Radiology,
Kobe University Graduate
School of Medicine,
Kobe, Hyogo, Japan

T. Itoh
Siemens Asahi Medical Technologies,
Tokyo, Japan

Abstract We evaluated quantification of calcified carotid stenosis by dual-energy (DE) CTA and dual-energy head bone and hard plaque removal (DE hard plaque removal) and compared the results to those of digital subtraction angiography (DSA). Eighteen vessels (13 patients) with densely calcified carotid stenosis were examined by dual-source CT in the dual-energy mode (tube voltages 140 kV and 80 kV). Head bone and hard plaques were removed from the dual-energy images by using commercial software. Carotid stenosis was quantified according to NASCET criteria on MIP images and DSA images at the same plane. Correlation between DE CTA and DSA was determined by cross tabulation. Accuracies for stenosis detection and grading were calculated. Stenosis could be evaluated in all vessels by DE CTA after applying DE hard plaque removal. In contrast, conventional CTA failed to show stenosis in 13 out of 18 vessels due to overlapping hard plaque. Good correlation between DE plaque removal images and DSA images was observed ($r^2=0.9504$) for stenosis grading. Sensitivity and specificity to detect hemodynamically relevant (>70%) stenosis was 100% and 92%, respectively. Dual-energy head bone and hard plaque removal is a promising tool for the evaluation of densely calcified carotid stenosis.

Keywords Dual-source CT · Carotid stenosis · Dual-energy CT · Carotid plaque · CTA

Introduction

Recent clinical trials have proven that the degree of the internal carotid artery stenosis is associated with cerebral stroke. According to the North American Symptomatic Carotid Endarterectomy Trial (NASCET) and the European Carotid Surgery Trial, symptomatic patients with severe stenoses (70–99%) can therefore benefit from carotid endarterectomy [1–3].

Conventional digital subtraction angiography (DSA) has been the "gold standard" for the evaluation of the degree of carotid artery stenosis, but conventional DSA has a tendency to underestimate the degree of carotid artery stenosis because it uses a limited number of projections and can therefore fail to detect the maximum internal carotid artery stenosis. 3D evaluation of carotid stenosis has become possible with rotation angiography, but this method remains invasive and is still associated with catheter-related complications.

Recently, noninvasive MR angiography (MRA) and CT angiography (CTA) have partially replaced conventional angiography [4–9] in particular since CTA correlates well

with catheter angiography and has high diagnostic accuracy for 70–99% stenosis. Moreover, high-quality DSA-like images can be generated with 3D CTA and maximum intensity projection (MIP) technique to gain an overview of the target vessel, which can help to detect maximum carotid stenosis. Nevertheless, CTA still shows a lower sensitivity for quantifying stenosis in the presence of dense calcification or indwelling stents since these may obscure contrast material in the lumen [10].

With dual-energy dual-source CT, two images can be simultaneously acquired with different tube voltages, corresponding to different X-ray energies. Materials can then be differentiated by analyzing their attenuation differences depending on tube voltage. The attenuation difference between two X-ray energies is especially large in materials with high atomic numbers such as iodine due to the photo effect, thus bones and calcified plaques, which show a smaller attenuation difference, can be distinguished from iodine [11, 12]. As a result, calcified plaque (hard plaque) can be removed from vessels with iodine contrast together with bone removal and quantification of carotid stenosis even in the presence of dense calcifications may become possible.

Here, we compared dual-energy head bone and hard plaque removal (DE hard plaque removal), applied to dual-energy CTA images, with conventional digital subtraction angiography (DSA) with a focus on quantification of calcified carotid artery stenosis.

Materials and methods

This study was performed after approval of the local institutional review board. Written informed consent was obtained from all patients. In the period between June 2007 and December 2007, 16 patients with internal carotid artery stenosis underwent both carotid DSA and carotid CTA by using dual-source CT with dual-energy mode. Calcium volume was calculated on precontrast images by using a workstation (Zio M900 Quadra, Ziosoft, Japan). Patients with noncalcified or slightly calcified carotid stenosis (calcium volume$\leq$50 mm^3) were excluded. Finally, 13 patients with densely calcified carotid stenosis (calcium volume$>$50 mm^3) were enrolled and a total of 18 vessels were analyzed. CT angiography was performed using a dual-source multidetector CT system (SOMATOM Definition, Siemens, Germany). The dual-energy mode was operated with the following CT parameters: tube voltages of 140 kV and 80 kV, tube current–time products of 90 effective mA s and 380 effective mA s, respectively, a rotation time of 0.5 s per rotation, 64×0.6-mm collimation with z-flying focal spot and a pitch of 0.6. The contrast bolus was chosen according to the patients' body weight as 1 ml/kg of contrast material (350 mg I/ml) and injected for 20 s via the antecubital vein followed by 25 ml of saline.

The delay before CT acquisition after injection was determined using bolus tracking software with a region of interest (ROI) was placed in a common carotid artery and a trigger threshold of 100 HU above the baseline. Two image datasets of different kV were reconstructed with 0.6-mm slice thickness and 0.6-mm slice gap. The reconstructed field of view was 200 mm. A soft convolution kernel (D30 kernel) was applied to obtain smooth 3D images. Dual-energy images of the carotids without bone and hard plaques were obtained from both datasets scanned at different tube voltage (Figs. 1 and 2) by using commercial postprocessing software (syngo 2008G, Siemens, Germany). We used the postprocessing software's default settings to remove cranial bone (head-bone removal). The combined images of both energy datasets were used for diagnostic reading and for 3D image (conventional CTA).
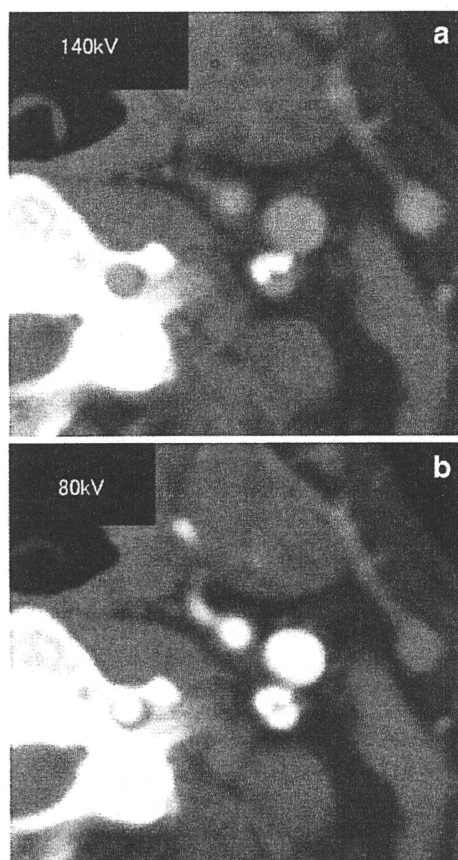
Fig. 1 Two images acquired by DSCT in the dual-energy mode at different tube voltages (140 kV and 80 kV) displayed with the same window width and window center (WW=600, WL=200). The densities of iodine and calcifications are higher in the 80-kV than in the 140-kV images, but the density difference of iodine between the 80-kV and 140-kV images is higher than that of calcifications